Molecular Orbital Studies of Zinc Oxide Chemical Vapor Deposition: Gas-Phase Hydrolysis of Diethyl Zinc, Elimination Reactions, and Formation of Dimers and Tetramers

Stanley M. Smith and H. Bernhard Schlegel*

Department of Chemistry, and Institute for Scientific Computing, Wayne State University, Detroit, Michigan, 48202

Received July 9, 2002. Revised Manuscript Received October 7, 2002

The chemical vapor deposition of zinc oxide thin films can be carried out with diethyl zinc and water vapor. The present study uses molecular orbital methods to examine complexes of one and two molecules of H_2O with $Zn(C_2H_5)_2$, and the subsequent hydrolysis, elimination, and oligomerization reactions which may occur in the gas phase. Geometry optimizations were carried out at the B3LYP/6-311G(d) level of theory. Hydrolysis of $Zn(C_2H_5)_2$ by a single water has an enthalpy barrier of 19 kcal/mol relative to separated reactants, which is reduced to 4 kcal/mol by the presence of a second water. Further hydrolysis of $Zn(C_2H_5)OH$ to $Zn(OH)_2$ is facile, but elimination of C_2H_6 or H_2O to form ZnO is very endothermic. $Zn(C_2H_5)OH$ and $Zn(OH)_2$ form very stable dimers and tetramers. Elimination of C_2H_6 and H_2O from the dimers and tetramers is also endothermic and leads to ring opening.

Introduction

Zinc oxide is a wide band gap semiconductor that is receiving increasing attention. Thin films have desirable properties such as good conductivity and high transparency in the visible region.[1,2] Doping with indium, gallium, or aluminum improves these properties.[3−5] These characteristics make zinc oxide thin films very suitable as transparent electrodes for solar cells and as replacements for tin oxide films.[1] Additional uses of zinc oxide films include thermoelectric devices, catalysts, piezoelectrics, and gas sensors.[6] Most recently, ultraviolet lasing has been observed in ZnO nanowires, nanoparticles, and thin films.[7−10] Zinc oxide thin films can be deposited by atmospheric pressure chemical vapor deposition (CVD) from dialkyl zinc and an oxygen source such as water in a temperature range of 350−500 °C.[3−5] High growth rates, excellent transparency, and good conductivity can be achieved by this approach. Films can also be grown from zinc acetate, $Zn(CH_3CO_2)_2$,[11] zinc acetylacetonate, $Zn(C_5H_7O_2)_2$,[12] and zinc amides[13] either by CVD or by spray pyrolysis. Water, peroxide, and alcohols are found to be more suitable oxygen sources than O_2, CO_2, or tetrahydrofuran. Zinc oxide films can also be deposited from alkylzinc alkoxides without an additional oxygen source.[14] There is some indication that gas-phase intermediates may be involved in ZnO film growth from dialkylzinc precursors,[5] and deposition from zinc acetate appears to have an activation energy of ca. 11 kcal/mol.[15]

For titanium nitride CVD, our computational studies and others have shown that typical gas-phase reactions contributing to the CVD process include association, ligand exchange, elimination, and oligomerization reactions.[16−18] Theoretical studies of gallium nitride CVD indicate similar reactions for this system as well.[19−21] Thus, we can anticipate that these reactions will also be important for zinc oxide CVD. Analogues of the dimeric and tetrameric zinc oxide species are known from experimental work in solution.[22] In this paper, we use density functional methods to explore some of the

(1) Gordon, R. G. *MRS Bull.* **2000**, *25*, 52−57.
(2) Gleizes, A. N. *Chem. Vapor Depos.* **2000**, *6*, 155−173.
(3) Hu, J. H.; Gordon, R. G. *J. Appl. Phys.* **1992**, *72*, 5381−5392.
(4) Hu, J. H.; Gordon, R. G. *J. Electrochem. Soc.* **1992**, *139*, 2014−2022.
(5) Hu, J. H.; Gordon, R. G. *J. Appl. Phys.* **1992**, *71*, 880−890.
(6) Hendrich, V. E.; Cox, P. A. *The Surface Science of Metal Oxides*; Cambridge University Press: Cambridge, U.K., 1994.
(7) Huang, M. H.; Mao, S.; Feick, H.; Yan, H.; Wu, Y.; Kind, H.; Weber, E.; Russo, R.; Yang, P. *Science* **2001**, *292*, 1897−1899.
(8) Cao, H.; Xu, J. Y.; Zhang, D. Z.; Chang, S. H.; Ho, S. T.; Seelig, E. W.; Liu, X.; Chang, R. P. H. *Phys. Rev. Lett.* **2000**, *84*, 5584−5587.
(9) Yu, P.; Tang, Z. K.; Wong, G. K. L.; Kawasaki, M.; Ohtomo, A.; Koinuma, H.; Segawa, Y. *J. Cryst. Growth* **1998**, *185*, 601−604.
(10) Bagnall, D. M.; Chen, Y. F.; Zhu, Z.; Yao, T.; Shen, M. Y.; Goto, T. *Appl. Phys. Lett.* **1998**, *73*, 1038−1040.
(11) Maruyama, T.; Shionoya, J. *J. Mater. Sci. Lett.* **1992**, *11*, 170−172.
(12) Minami, T.; Sonohara, H.; Takata, S.; Sato, H. *Jpn. J. Appl. Phys.* **1994**, *33*, L743−L746.
(13) Suh, S.; Miinea, L. A.; Hoffman, D. M.; Zhang, Z.; Chu, W. K. *J. Mater. Sci. Lett.* **2001**, *20*, 115−118.
(14) Auld, J.; Houlton, D. J.; Jones, A. C.; Rushworth, S. A.; Malik, M. A.; Obrien, P.; Critchlow, G. W. *J. Mater. Chem.* **1994**, *4*, 1249−1253.
(15) Jain, S.; Kodas, T. T.; Hampden-Smith, M. *Chem. Vapor Depos.* **1998**, *4*, 51−59.
(16) Cundari, T. R.; Morse, J. M. *Chem. Mater.* **1996**, *8*, 189−196.
(17) Baboul, A. G.; Schlegel, H. B. *J. Phys. Chem. B* **1998**, *102*, 5152−5157.
(18) Cross, J. B.; Schlegel, H. B. *Chem. Mater.* **2000**, *12*, 2466−2474.
(19) Timoshkin, A. Y.; Bettinger, H. F.; Schaefer, H. F. *J. Cryst. Growth* **2001**, *222*, 170−182.
(20) Watwe, R. M.; Dumesic, J. A.; Kuech, T. F. *J. Cryst. Growth* **2000**, *221*, 751−757.
(21) Nakamura, K.; Makino, O.; Tachibana, A.; Matsumoto, K. *J. Organomet. Chem.* **2000**, *611*, 514−524.
(22) Kuran, W.; Czernecka, M. *J. Organomet. Chem.* **1984**, *263*, 1−7.

10.1021/cm020726p CCC: $25.00
Published on Web 11/16/2002

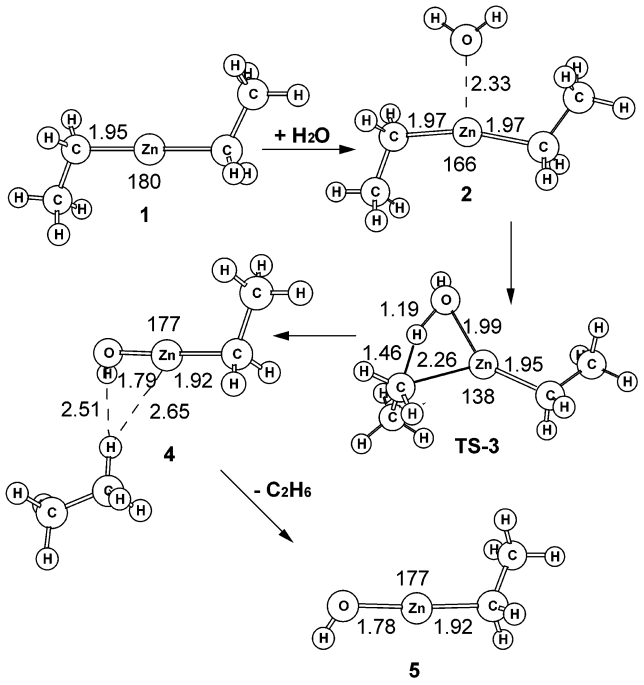

Figure 1. Optimized geometries for $Zn(C_2H_5)_2$ reacting with one molecule of H_2O.

possible mechanisms for the gas-phase reaction for $Zn(C_2H_5)_2 + H_2O$ and the formation of clusters.

Method

Molecular orbital calculations were carried out using the development version of the GAUSSIAN series of programs.[23] Equilibrium geometries were optimized by the B3LYP density functional method[24−26] using the 6-311G(d) basis set[27−31] (for zinc, this corresponds to the 14s,9p,5d Wachters−Hay basis set[29−31] contracted to 9s,5p,3d and augmented with an f-type Gaussian shell with an exponent of 1.620). Similar to the work on titanium nitride CVD reactions,[16−18] the B3LYP/6-311G(d) energy differences in the present work are anticipated to have a mean absolute deviation of 5 kcal/mol or less when compared to experimental values. Vibrational frequencies were computed at this level of theory and were used without scaling because the B3LYP frequencies agree quite well with experimental values for a wide range of second- and third-period compounds.[32] Zero-point energies, thermal corrections, and entropies were calculated by standard statistical thermodynamic methods[33] using the unscaled B3LYP frequencies and the ideal gas/rigid rotor/harmonic oscillator approximations.

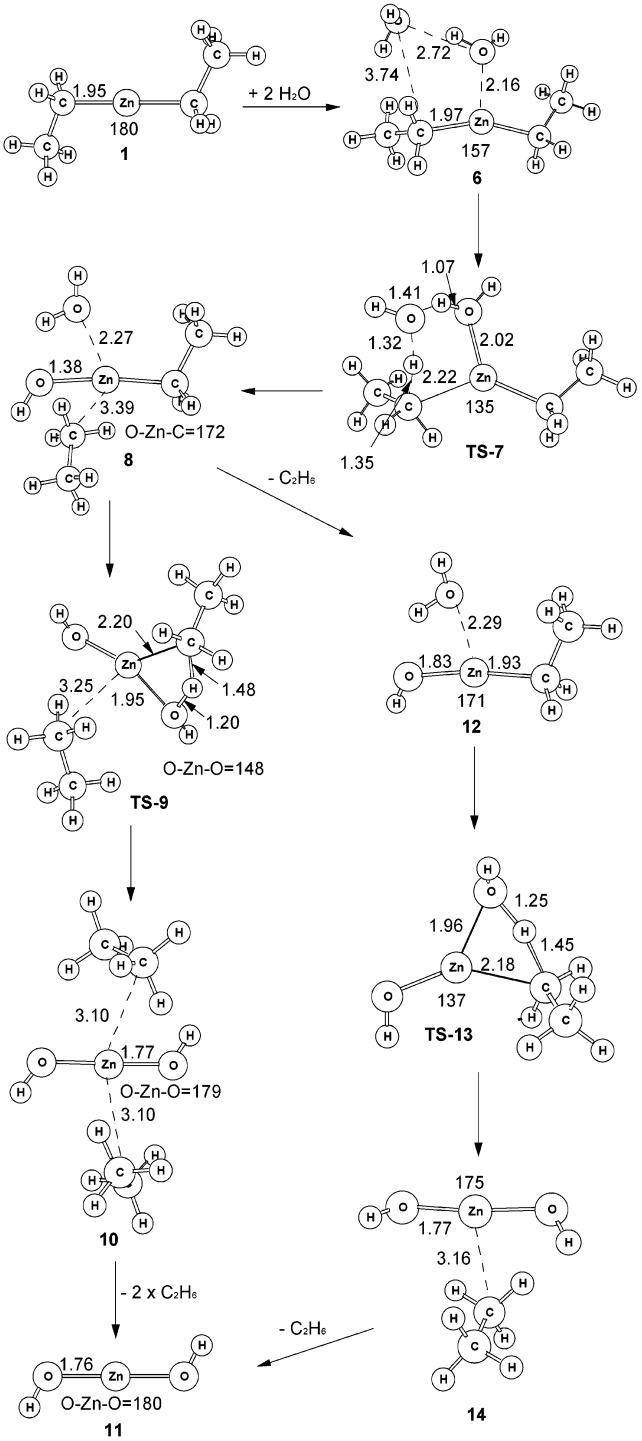

Figure 2. Optimized geometries for $Zn(C_2H_5)_2$ reacting with two molecules of H_2O.

Results and Discussion

The first steps in the chemical vapor deposition of zinc oxide thin films from diethyl zinc is most likely the partial or complete hydrolysis of $Zn(C_2H_5)_2$. The struc-

(23) Frisch, M. J.; Trucks, G. W.; Schlegel, H. B.; Scuseria, G. E.; Robb, M. A.; Cheeseman, J. R.; Zakrzewski, V. G.; Montgomery, J. A.; Stratmann, R. E.; Burant, J. C.; Dapprich, S.; Millam, J. M.; Daniels, A. D.; Kudin, K. N.; Strain, M. C.; Farkas, O.; Tomasi, J.; Barone, V.; Cossi, M.; Cammi, R.; Mennucci, B.; Pomelli, C.; Adamo, C.; Clifford, S.; Ochterski, J.; Petersson, G. A.; Ayala, P. Y.; Cui, Q.; Morokuma, K.; Malick, D. K.; Rabuck, A. D.; Raghavachari, K.; Foresman, J. B.; Cioslowski, J.; Ortiz, J. V.; Stefanov, B. B.; Liu, G.; Liashenko, A.; Piskorz, P.; Komaromi, I.; Gomperts, R.; Martin, R. L.; Fox, D. J.; Keith, T.; Al-Laham, M. A.; Peng, C. Y.; Nanayakkara, A.; Gonzalez, C.; Challacombe, M.; Gill, P. M. W.; Johnson, B. G.; Chen, W.; Wong, M. W.; Andres, J. L.; Head-Gordon, M.; Replogle, E. S.; Pople, J. A. GAUSSIAN (development version); Gaussian, Inc.: Pittsburgh, PA.
(24) Becke, A. D. *Phys. Rev. A* **1988**, *38*, 3098−3100.
(25) Becke, A. D. *J. Chem. Phys.* **1993**, *98*, 5648−5652.
(26) Lee, C.; Yang, W.; Parr, R. D. *Phys. Rev. B* **1988**, *37*, 785−789.
(27) Krishnan, R.; Binkley, J. S.; Seeger, R.; Pople, J. *J. Chem. Phys.* **1980**, *72*, 650.
(28) McLean, A. D.; Chandler, G. S. *J. Chem. Phys.* **1980**, *72*, 5639.
(29) Wachters, A. J. H. *J. Chem. Phys.* **1970**, *52*, 1033.
(30) Hay, J. P. *J. Chem. Phys.* **1977**, *66*, 4377.
(31) Raghavachari, K.; Trucks, G. W. *J. Chem. Phys.* **1989**, *91*, 1062.
(32) Scott, A. P.; Radom, L. *J. Phys. Chem.* **1996**, *100*, 16502−16513.
(33) McQuarrie, D. A. *Statistical Thermodynamics*; University Science Books: Mill Valley, CA, 1973.

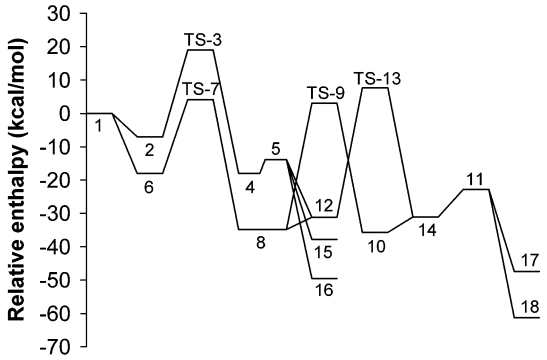

Figure 3. Enthalpy profile for the hydrolysis of $Zn(C_2H_5)_2$ computed at the B3LYP/6-311G(d) level of theory.

tures along these paths are shown in Figures 1 and 2, and the enthaply profiles for these reactions are summarized in Figure 3. The $Zn(C_2H_5)OH$ and $Zn(OH)_2$ produced in the hydrolysis can form dimers, tertamers, or higher oligomers as outlined in Figures 4 and 5, and these can potentially eliminate C_2H_6 or H_2O to yield Zn_nO_n. The relative enthalpies, free energies, and absolute entropies are listed in Table 1.

Single Hydrolysis. Diethyl zinc, **1**, has a linear C−Zn−C angle and little or no barrier for rotation about the Zn−C bonds. Complexation with a molecule of water yields structure **2**, which lies 7 kcal/mol below the reactants. As shown in Figure 1, the water is located with the oxygen pointing toward the zinc in the middle of the molecule at a distance of 2.33 Å. The complex has C_s symmetry and the C−Zn−C angle has changed from 180° to 166° with the ethyl ligands moving away from the water. The single hydrolysis transition state, **TS-3**, is 19 kcal/mol above the reactants. The transition vector is dominated by the motion of the hydrogen, which is 1.19 Å from the oxygen and 1.46 Å from the carbon. The Zn−O bond is nearly fully formed (1.99 Å vs 1.78 Å in $Zn(C_2H_5)OH$), and the Zn−C bond is substantially elongated (2.26 Å vs 1.95 Å in $Zn(C_2H_5)_2$). The post-transition-state complex, **4**, lies at −18 kcal/mol relative to reactants, and the ethane is bound by ca. 4 kcal/mol. One of the C−H bonds of ethane points toward the Zn−O bond at a distance of ca. 2.5 Å; the remainder of the structure is essentially the same as the dissociated product, **5**. The hydrolysis product, $Zn(C_2H_5)OH$, **5**, lies 14 kcal/mol below the reactants. The C−Zn−O angle is nearly linear and the Zn−C and Zn−O bond lengths are similar to those in $Zn(C_2H_5)_2$ and $Zn(OH)_2$.

Double Hydrolysis. The complex with two waters bound to diethyl zinc, **6**, is 18 kcal/mol below the reactants. As illustrated in Figure 2, the two waters are on the same side of diethyl zinc and hydrogen-bonded to each other. The transition state **TS-7** lies 4 kcal/mol above the reactants and involves a proton relay. Similar to the transitions state for hydrolysis by a single water, the bond between the zinc and the hydroxyl group of the first water in **TS-7** is well formed, with a distance of 2.02 Å. This water is beginning to transfer a proton to the second water, which in turn transfers one of its protons to the leaving ethyl group. This second proton is approximately midway between the oxygen and carbon, and its motion dominates the transition vector. As in the hydrolysis involving a single molecule of water, the Zn−C bond is nearly broken, with the leaving ethane 2.22 Å away from zinc. The post-transition-state complex, **8**, lies 35 kcal/mol below the reactants. It can also be reached by water-binding to the single hydrolysis complex, **4**. The water is bound by 17 kcal/mol, and sits 2.27 Å from zinc with a hydrogen bond to the oxygen of $Zn(C_2H_5)OH$. Similar to **4**, the ethane in **8** is bound by

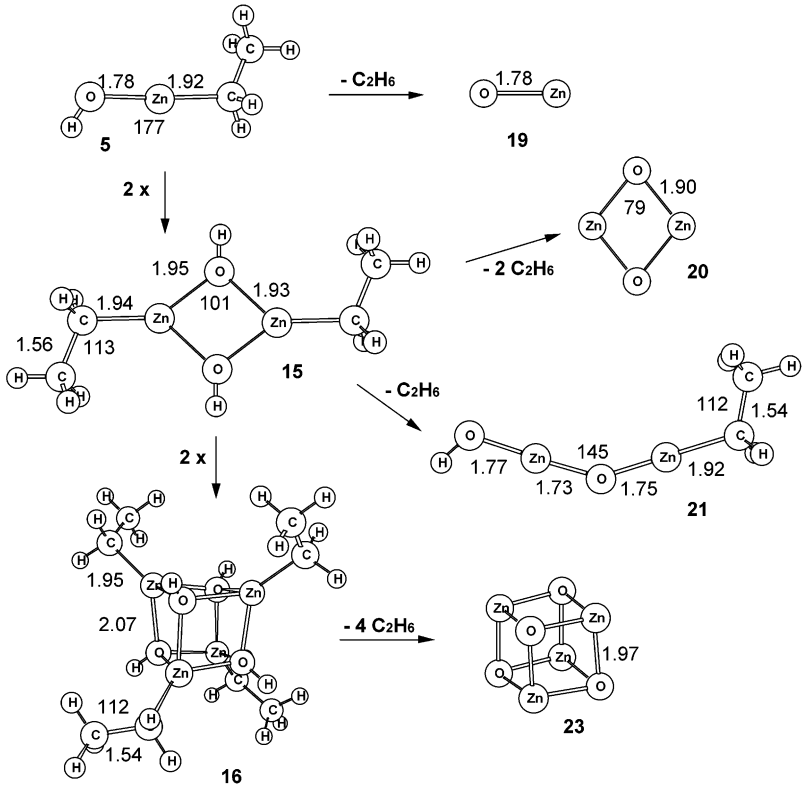

Figure 4. Optimized geometries and enthalpies for the formation of dimers and tetramers of $Zn(C_2H_5)OH$, and subsequent elimination reactions.

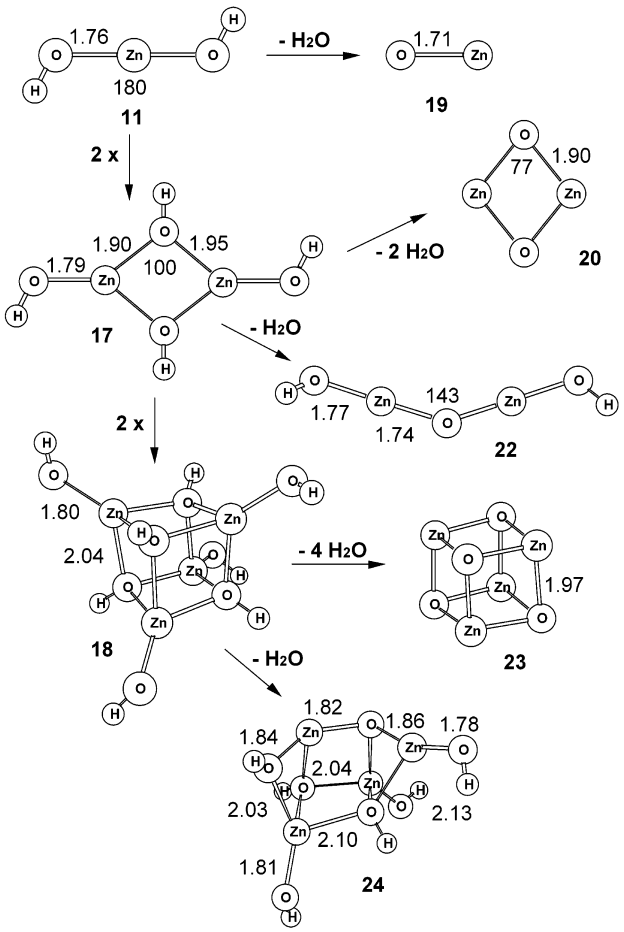

Figure 5. Optimized geometries and enthalpies for the formation of dimers and tetramers of $Zn(OH)_2$, and subsequent elimination reactions.

only 4 kcal/mol, and one of the C−H bonds points toward the Zn−O bond at a distance of ca. 2.5 Å. From **8**, the reaction can proceed to the second hydrolysis transition state, **TS-9**, which lies 3 kcal/mol above the reactants. The distances for the bonds being made and broken are very similar to those of the other hydrolysis transition states. The post-transition-state complex **10** lies 36 kcal/mol below the reactants. The dissociation of the two ethanes from **10** leads to the double hydrolysis product $Zn(OH)_2$, **11**, which is 23 kcal/mol below the reactants. An alternate pathway involves the dissociation of ethane from complex **8** to yield $Zn(C_2H_5)OH{\cdot}H_2O$, **12**. Complex **12** can also be formed from the addition of water to **5**, and has a water binding energy of 17 kcal/mol. The geometry of the transition state for this hydrolysis, **TS-13**, is nearly identical to that of **TS-9**, but is ca. 5 kcal/mol higher, which corresponds to the C_2H_6 binding energy in **TS-9**. The ethane in the post-transition-state complex is bound by ca. 8 kcal/mol and has a C−H bond pointing to each of the oxygens in $Zn(OH)_2$.

Dimer and Tetramer of $Zn(C_2H_5)OH$. As shown in Figure 4, the simplest case for oligomerization is the formation of the zinc ethyl hydroxide dimer, **15**, from two zinc ethyl hydroxide molecules, which is exothermic by 48 kcal/mol. The reaction path optimization method[34] showed that the dimerization reaction is barrierless.

(34) Ayala, P. Y.; Schlegel, H. B. *J. Chem. Phys.* **1997**, *107*, 375−384.

Table 1. Enthalpies, Free Energies, and Entropies Computed at the B3LYP/6-311G(d) Level of Theory[a]

structure	ΔH_{298}	ΔG_{700}	structure	S_{298}
1 + 2 H_2O	0.0	0.0	**1**	89.0
2 + H_2O	−7.0	11.3	**2**	109.9
TS-3 + H_2O	19.1	42.4	**TS-3**	103.3
4 + H_2O	−17.9	−1.3	**4**	112.7
5 + H_2O + C_2H_6	−13.8	−20.8	**5**	80.9
6	−18.0	30.5	**6**	119.8
TS-7	4.2	54.7	**TS-7**	118.0
8	−34.8	11.8	**8**	123.7
TS-9	3.1	50.0	**TS-9**	122.7
10	−35.6	8.5	**10**	126.5
11 + 2 C_2H_6	−22.7	−31.3	**11**	71.0
12 + C_2H_6	−31.1	−9.3	**12**	93.4
TS-13 + C_2H_6	7.7	31.2	**TS-13**	90.6
14 + C_2H_6	−31.0	−12.5	**14**	97.6
$^1/_2$ **15** + H_2O + C_2H_6	−37.8	−28.1	**15**	121.9
$^1/_4$ **16** + H_2O + C_2H_6	−49.4	−28.4	**16**	187.0
$^1/_2$ **17** + 2 C_2H_6	−47.3	−39.5	**17**	102.2
$^1/_4$ **18** + 2 C_2H_6	−61.3	−42.3	**18**	154.1
19 + H_2O + 2 C_2H_6	78.8	44.7	**19**	53.9
$^1/_2$ **20** + H_2O + 2 C_2H_6	31.9	13.0	**20**	72.7
$^1/_2$ **21** + H_2O + $^3/_2$ C_2H_6	−18.0	−25.1	**21**	104.4
$^1/_2$ **22** + $^1/_2$ H_2O + 2 C_2H_6	−22.6	−29.4	**22**	91.1
$^1/_4$ **23** + H_2O + 2 C_2H_6	−1.8	−10.7	**23**	96.2
$^1/_4$ **24** + $^1/_4$ H_2O + 2 C_2H_6	−46.4	−35.8	**24**	143.1

[a] Enthalpies and free energies in kcal/mol, entropies in cal/mol degree; enthalpies and entropies at 298.15 K, 1 atm; free energies at 700 K, 10 Torr.

This dimer contains a planar Zn_2O_2 ring with C_{2h} symmetry and has Zn−O bond lengths of 1.93 and 1.95 Å. The carbons of the ethyl groups and the hydrogens bonded to oxygens are also in the plane of the ring. Two of these dimers can react further to form a tetramer, **16**. This reaction is barrierless and exothermic by 47 kcal/mol. The eight atoms of the cube structure have nearly equal ZnO bond lengths of ca. 2.07 Å. The top four atoms are slightly twisted from the bottom four by an angle of 6.9°. Similar tetramers have been seen in solution.[22]

Dimer and Tetramer of $Zn(OH)_2$. The formation of the $Zn_2(OH)_4$ and $Zn_4(OH)_8$ from $Zn(OH)_2$ is shown in Figure 5. Both reactions are barrierless and a little more exothermic than the zinc ethyl hydroxide case. The dimer structure **17** contains a planar ring and lies 49 kcal/mol below 2 $Zn(OH)_2$. The Zn−O bonds in the ring have significantly different lengths, 1.90 and 1.95 Å; probably due to an interaction with the lone pair of the exocyclic oxygen. Two of these dimers can react further without a barrier to form a tetramer, **18**, which lies 52 kcal/mol below 2 $Zn_2(OH)_4$. The eight atoms form a distorted cube with bond lengths of ca. 2.04 Å. Even in the small clusters considered in this study, the average Zn−O bond lengths of the monomer (1.78 Å), dimer (1.93 Å), and tetramer (2.02 Å) of zinc hydroxide uniformly approach the Zn−O distance in the solid (2.14 Å obtained from the sum of ionic radii).

Elimination Reactions. To form a zinc oxide film, additional ligands must be eliminated from the complexes discussed so far. For the monomers, elimination of C_2H_6 from $Zn(C_2H_5)OH$ or H_2O from $Zn(OH)_2$ yields ZnO. However, these reactions are rather endothermic (>50 kcal/mol) and will not occur in the gas phase. Eliminating two molecules of C_2H_6 from dimer **15** (Figure 3) or two H_2O from **17** leading to Zn_2O_2, **20**, is also very endothermic (>100 kcal/mol). Removal of one ethane from **15** requires 40 kcal/mol and results in ring

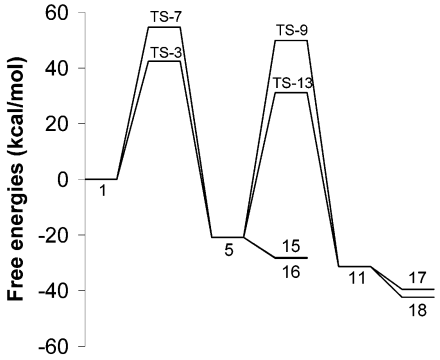

Figure 6. Free energy profile for the hydrolysis of $Zn(C_2H_5)_2$ computed at the B3LYP/6-311G(d) level of theory.

opening, **21** (Figure 4). Similarly, removal of one water from **17** requires 49 kcal/mol and produces the ring-opening product **22** (Figure 5). Ring closure was not observed for either complex.

If elimination from the monomer or the dimer are unfavorable, perhaps the tetramer may be more favorable. As illustrated in Figures 4 and 5, removal of four ethanes from **16** or of four waters from **18** leads to Zn_4O_4, **23**, which has a cubic structure that resembles a solid. However, this process requires nearly 200 kcal/mol. Removal of only one molecule of water from tetramer **18** requires 60 kcal/mol, and leads to ring opening, **24**, analogous to elimination reactions from the dimers, **15** → **21** and **17** → **22**. This suggests that the tetramers or possibly larger oligomers may be stable enough to be observed in the gas phase, similar to those seen in solution.[22]

Enthalpies, Free Energies, and Rate Constants

Table 1 and Figure 3 summarize the enthalpy changes for the gas-phase hydrolysis. The pathway involving two water molecules in a catalytic fashion, **1** → **TS-7** → **8** → **TS-9** → **11**, is favored in terms of enthalpy over a sequential mechanism involving one water at a time, **1** → **TS-3** → **5** → **TS-13** → **11**. However, at typical experimental conditions (700 K and 10 torr), most of the complexes are not bound in terms of free energy. As shown in Figure 6, both hydrolysis steps have negative free energies of reaction. Relative to the reactants, the first hydrolysis remains higher, but the uncatalyzed reaction, **TS-3**, is ca. 10 kcal/mol lower than the catalyzed reaction, **TS-7**. Likewise, the second hydrolysis proceeds through the uncomplexed transition state, **TS-13**. The formation of the dimers and tetramers is strongly favored in terms of enthalpy, but only modestly in free energy. Structure **18**, the tetramer of $Zn(OH)_2$, is the most stable structure computed in this study and resembles clusters seen in solution. Gas-phase elimination reactions for the dimers and tetramers are endothermic in both enthalpy and free energy, and lead to ring opening. Perhaps elimination to form Zn_nO_n clusters may become more favorable for larger oligomers when the number of ligands around the zinc and the oxygen is closer to that found in the bulk.

Transition state theory can be used to estimate the reaction rates, $k = (k_B T/h) \exp(-\Delta G^{\circ\ddagger}/RT)$ using 1 mol L^{-1} as the standard state; however, absolute reaction rates are quite sensitive to the accuracy of the barrier height. At 700 K, the rate constant for the first hydrolysis is ca. $2.05 \times 10^5 = 2.30 \times 10^{12} \exp(-22.57 \text{ kcal mol}^{-1}/RT)$ L mol^{-1} s^{-1} via transition state **TS-3**, and ca. $1.03 \times 10^5 = 1.34 \times 10^8 \exp(-9.65 \text{ kcal mol}^{-1}/RT)$ L^2 mol^{-2} s^{-1} via transition state **TS-7** which involves a complex with an additional water. For the second hydrolysis step, the rate constants are ca. $3.72 \times 10^3 = 2.25 \times 10^{11} \exp(-24.93 \text{ kcal mol}^{-1}/RT)$ L mol^{-1} s^{-1} for the reaction via the uncomplexed transition state **TS-13**, and ca. $2.26 \times 10^1 = 4.15 \times 10^8 \exp(-23.26 \text{ kcal mol}^{-1}/RT)$ L^2 mol^{-2} s^{-1} via **TS-9**. At typical CVD conditions with low concentrations of water, the hydrolysis proceeds in two steps, and does not involve complexation with an additional molecule of water.

Conclusions

In this paper we have characterized some of the probable intermediates and pathways for gas-phase reactions involved in zinc oxide chemical vapor deposition. Hydrolysis of diethyl zinc proceeds stepwise, and under typical CVD conditions does not involve catalysis by additional water molecules. Partially and fully hydrolyzed intermediates can readily form dimers and tetramers. Elimination reactions from these small clusters to form Zn_2O_2 and Zn_4O_4 are energetically unfavorable, but may become feasible for larger oligomers.

Acknowledgment. We gratefully acknowledge support from the National Science Foundation (CHE 0131157) and from the National Computational Science Alliance under CHE980042N utilizing the NCSA HP Exemplar SPP-2000.

CM020726P